Cell

# Hippo Pathway Activity Influences Liver Cell Fate

Dean Yimlamai,[1,2,8] Constantina Christodoulou,[1,3,4,8] Giorgio G. Galli,[1,3,4] Kilangsungla Yanger,[5] Brian Pepe-Mooney,[1,3,4] Basanta Gurung,[1,3,4] Kriti Shrestha,[1] Patrick Cahan,[1] Ben Z. Stanger,[5,6,7] and Fernando D. Camargo[1,3,4,*]
[1]The Stem Cell Program, Boston Children's Hospital, Boston, MA 02115, USA
[2]Division of Gastroenterology and Nutrition, Department of Medicine, Boston Children's Hospital, Boston, MA 02115, USA
[3]Harvard Stem Cell Institute, Cambridge, MA 02138, USA
[4]Department of Stem Cell and Regenerative Biology, Harvard University, Cambridge, MA 02138, USA
[5]Department of Medicine, Gastroenterology Division
[6]Abramson Family Cancer Research Institute
[7]Department of Cell and Developmental Biology
Perelman School of Medicine, University of Pennsylvania, Philadelphia, PA 19104, USA
[8]Co-first author
*Correspondence: fernando.camargo@childrens.harvard.edu
http://dx.doi.org/10.1016/j.cell.2014.03.060

## SUMMARY

**The Hippo-signaling pathway is an important regulator of cellular proliferation and organ size. However, little is known about the role of this cascade in the control of cell fate. Employing a combination of lineage tracing, clonal analysis, and organoid culture approaches, we demonstrate that Hippo pathway activity is essential for the maintenance of the differentiated hepatocyte state. Remarkably, acute inactivation of Hippo pathway signaling in vivo is sufficient to dedifferentiate, at very high efficiencies, adult hepatocytes into cells bearing progenitor characteristics. These hepatocyte-derived progenitor cells demonstrate self-renewal and engraftment capacity at the single-cell level. We also identify the NOTCH-signaling pathway as a functional important effector downstream of the Hippo transducer YAP. Our findings uncover a potent role for Hippo/YAP signaling in controlling liver cell fate and reveal an unprecedented level of phenotypic plasticity in mature hepatocytes, which has implications for the understanding and manipulation of liver regeneration.**

## INTRODUCTION

The liver has a tremendous latent regenerative capacity. Within a few days, 90% of the liver mass lost to a partial hepatectomy can be restored by hepatocyte proliferation of the remaining liver lobes. Under conditions of extreme stress or chronic injury, a population of atypical ductal cells, usually referred to as ''oval cells,'' emerges from the bile ducts and is thought to participate in liver repair (Oertel and Shafritz, 2008; Turner et al., 2011). These putative hepatic progenitor cells are able to differentiate into hepatocytes and biliary cells as evidenced by lineage tracing studies after injury (Espanol-Suner et al., 2012; Huch et al., 2013). However, the fate relationships between hepatocytes, ductal cells, and progenitors are still unclear and highly debated (Greenbaum, 2011; Michalopoulos, 2012). Also lacking is the identification of signaling pathways that specify and maintain progenitor fate within the liver.

The Hippo/YAP-signaling pathway is a critical regulator of liver size (Camargo et al., 2007; Dong et al., 2007). Hippo pathway signaling engagement results in phosphorylation and inactivation of the transcriptional coactivator YAP (Ramos and Camargo, 2012). Components of this signaling cascade include the tumor suppressor NF2, the scaffolding molecule WW45, the *Drosophila Hippo* orthologs MST1/2, and their substrates, the kinases, LATS1/2. YAP phosphorylation by LATS1/2 results in its cytoplasmic localization and proteolytic degradation (Oka et al., 2008; Zhao et al., 2007). YAP exerts its transcriptional activity mostly by interacting with the TEAD family of transcription factors and activating target gene expression (Wu et al., 2008; Zhang et al., 2008). Manipulation of Hippo pathway activity leads to profound changes in liver cell proliferation. YAP overexpression results in approximately a 4-fold increase in liver size within weeks (Camargo et al., 2007; Dong et al., 2007). Additionally, acute postnatal loss of *Mst1/2* (Zhou et al., 2009), *Nf2* (Benhamouche et al., 2010), and *Ww45* (Lee et al., 2010) leads to increased YAP levels, resulting in hepatomegaly and eventually liver cancer. In most of these models, the presence of a large number of atypical ductal cells has led to the prevailing view that overgrowth in these models is mostly driven by the activation and expansion of putative progenitors (Benhamouche et al., 2010). However, given that genetic manipulations in these mice occurred in all liver populations (hepatocytes, ductal cells, and progenitors), it is still unknown which cell types within the liver respond to alterations in Hippo signaling. Furthermore, the identity of the functional YAP transcriptional targets that drive these responses remain to be elucidated.

Here, we demonstrate that Hippo/YAP signaling plays an essential role by determining cellular fates in the mammalian liver. Elevated YAP activity defines hepatic progenitor identity and its ectopic activation in differentiated hepatocytes results in their

dedifferentiation, driving liver overgrowth and "oval" cell appearance. Our data identify the NOTCH-signaling pathway as one important downstream target of YAP in liver cells. Our work also uncovers a remarkable plasticity of the mature hepatocyte state.

## RESULTS

### YAP Is Enriched and Activated in the Biliary Compartment

The identity of the Hippo-responsive cells within the liver is unclear. To bring insight into this question, we analyzed Hippo pathway signaling activity in the epithelial compartments of the mammalian liver. YAP is expressed at high levels in bile ducts, with many ductal cells displaying robust nuclear YAP localization (Figure 1A). YAP protein is detected at lower levels in hepatocytes (Li et al., 2011; Zhang et al., 2010), where the signal is diffuse throughout the cell (Figure 1A). Immunohistochemical (IHC) analysis of livers with a mosaic deletion of YAP confirms this observation (Figure 1A, right panel). Immunoblot analyses confirm higher levels of YAP protein in purified ductal cells and also indicate a robust decrease in relative phospho-YAP levels (Figure 1B). Gene expression analysis of isolated hepatocytes versus sorted ductal cells further demonstrates a marked enrichment of YAP/TEAD target genes, as well as of *Yap1* itself, in the ductal fraction (Figure 1C; Figure S1A available online).

To extend these observations, we generated mice with a bacterial artificial chromosome (BAC) knockin of EGFP in the connective tissue growth factor gene (*Ctgf*) locus. *Ctgf* is the most highly characterized YAP target gene (Lee et al., 2010; Lu et al., 2010). In support of our staining data, we find that EGFP expression is absent in hepatocytes and is restricted to a subset of ductal cells expressing the markers CK19, SOX9, and A6 (Figure 1D), which have been historically associated with hepatic progenitors and the ductal fate (Demetris et al., 1996; Dorrell et al., 2011; Engelhardt et al., 1993). CTGF protein was also enriched in biliary cell lysates (Figure 1B), confirming enhanced YAP transcriptional activity in this cellular compartment. Thus, our results demonstrate that YAP activity and expression is highly enriched in a subset of ductal cells expressing markers associated with progenitor cells. On the other hand, mature hepatocytes display higher Hippo pathway activity as YAP nuclear levels and transcriptional activity are reduced.

### YAP Activation Induces a Ductal Fate in Hepatocytes

We then sought to evaluate the differential effects of Hippo/YAP manipulation in hepatocytic and ductal/progenitor cellular compartments in vivo. These experiments would provide insight into the nature of the cell type(s) that respond to YAP and are responsible for liver overgrowth.

We first utilized a *Ck19-CreERT* driver to activate expression of a doxycycline (Dox)-inducible version of human YAP carrying an S127A mutation (TetOYAP; Figure S1B). This protein has enhanced nuclear localization by escaping inactivation by LATS1/2 (Zhao et al., 2007). Tamoxifen injection into mice followed by Dox administration leads to mosaic activation of transgenic YAP (Figure S1B). Cells expressing the transgene can be visualized given that the YAP antibody used has a much higher affinity for human YAP. Two weeks post-Dox, YAP transgene-expressing (Tg) CK19+ cells appeared to take on a rounded morphology that distinguished these cells from the remainder of the cuboidal biliary epithelium (Figure S1B). Four and eight weeks post-Dox, larger groups of cells appeared to grow within the ductal epithelium, occasionally forming multilayered structures (Figure S1B). Because putative liver progenitors are known to express CK19, we hypothesized that YAP expression would expand such a cell population and mimic an atypical ductular reaction, where progenitors exit out of the portal area and enter into the hepatic parenchyma (Demetris et al., 1996). No such cells were identified, suggesting that expression of activated YAP in the biliary/progenitor compartment results in ductal hyperplasia but does not result in progenitor activation or in their entry into the hepatocyte compartment.

Directed hepatocyte-specific activation of YAP was achieved by administering a Cre-expressing adenoassociated virus (AAV-Cre) to TetOYAP mice (Figure 1E). AAV2/8 preferentially targets hepatocytes and is currently the method of choice for gene delivery to this cell type (Fan et al., 2012; Malato et al., 2011). Furthermore, this vector's cell-type specificity was improved by using a liver-specific promoter to drive Cre (Tanigawa et al., 2007). We validated the hepatocyte specificity of this virus by immunofluorescence examination of tissues (Figure S1C) and by fluorescence-activated cell sorting (FACS) analysis of isolated hepatocyte and ductal fractions (Figure S1D). Additionally, we generated liver organoids from Cre-reporter mice infected with AAV-Cre to determine if any organoid-forming progenitors would be infected with the virus (Huch et al., 2013) (Figure S1E). Combined, these analyses confirmed the previously reported hepatocyte specificity of AAV-Cre, although it suggested that an extremely low fraction (0.2%–0.5%) of progenitors/ductal cells could be infected at high AAV-Cre doses.

TetOYAP mice that were exposed to AAV-Cre, but were not given Dox, had normal appearing livers (Figure 1F). In contrast, AAV-Cre-treated TetOYAP mice given Dox for 3 weeks had a rapid increase in liver growth (Figures 1F and S1F). Surprisingly, histological analyses of +Dox livers revealed the widespread appearance of small cells with scant cytoplasm, to the extent that up to 80% of the liver was composed of this cell population (Figure 1F). This cellular morphology was highly reminiscent of putative progenitors associated with typical ductular reactions. IHC characterization of Tg livers revealed strikingly broad expression of the ductal markers pan-cytokeratin (panCK) and HNF1β (Figure 1G). Additionally, livers were overwhelmingly positive for SOX9 (Figure 1G), whose expression was initially more prominent around portal as compared to central venous areas (Figure S1G). Likewise, the initial wave of proliferation was primarily centered on portal areas as identified by phospho-Histone H3 staining (Figure S1H). Overall, our data suggest that YAP activation in hepatocytes leads to overgrowth and the emergence of cells bearing characteristics of ductal/progenitor cells. In contrast, YAP activation in the ductal compartment cells leads to hyperplasia, but not to an oval-cell-like appearance.

### YAP Activation Dedifferentiates Single Adult Hepatocytes

Our data above could be explained by two possibilities: either YAP activation dedifferentiates hepatocytes into

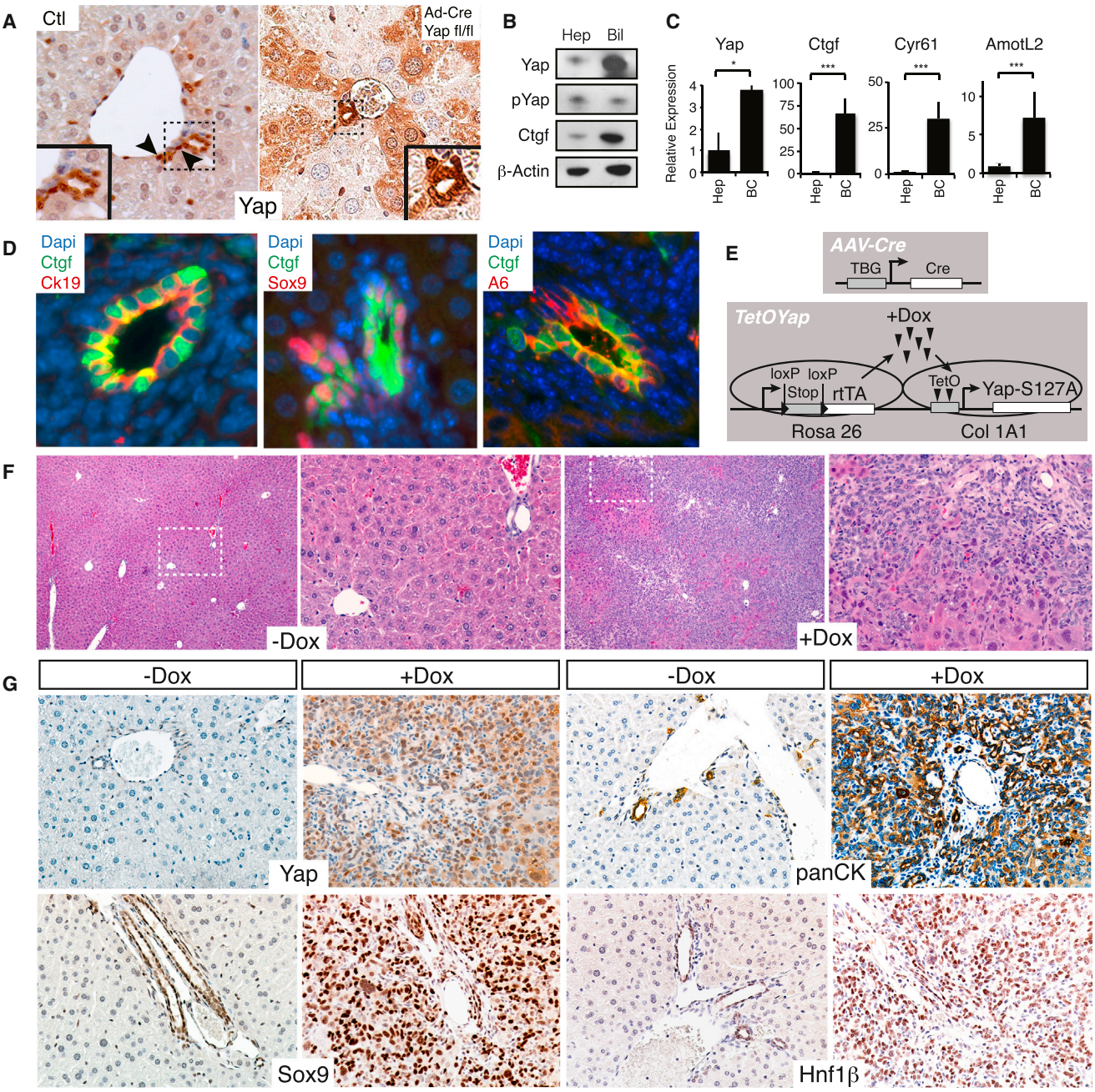


**Figure 1. Hepatocyte-Specific YAP Expression Results in Ductal/Progenitor Marker Expression**

(A) YAP protein/activity is enriched in a subset of ductal cells. Control (Ctl) liver YAP staining (400×) shows prominent signaling in bile ductules. Arrowheads indicate ductal cells with nuclear YAP (inset shows magnified view). *Yap*$^{fl/fl}$ mice given Ad-Cre recombinase (Ad-cre *Yap*$^{fl/fl}$) demonstrate patchy YAP staining in hepatocytes (100×).

(B) Immunoblots of human hepatocyte (Hep) and biliary (Bil) lysates for YAP, pYAP, CTGF, and β-actin.

(C) Quantitative real-time PCR comparing relative levels of YAP and YAP targets in hepatocytes (Hep) and biliary cells (BC). n = 3; mean ± SEM.

(D) *Ctgf-EGFP* mice show EGFP costaining (Ctgf) in a subset of CK19, SOX9, and A6-expressing cells.

(E) Experimental design for hepatocyte-specific YAP overexpression.

(F) Hematoxylin and eosin (H&E) of uninduced (−Dox) or YAP Tg mouse (+Dox) for 21 days following injection with $10^{11}$ plaque-forming units (pfu) of AAV-Cre. Right image displays a magnification of inset.

(G) Representative immunohistochemical stains of portal areas for YAP, panCK, SOX9, and HNF1β for the mice displayed in (F). *p < 0.05; ***p < 0.001.

See also Figure S1.

progenitor/ductal-like cells or YAP activation leads to recruitment and/or expansion of a progenitor/ductal population. To distinguish between these two possibilities, we titrated the viral titer down such that individual hepatocytes could be infected and fate mapped for months without interference from neighboring clones (Figure 2A). Additionally, for many of these experiments, we utilized a Cre-dependent reporter to faithfully assess the cell autonomy of this phenotype. Microscopic examination of mouse livers given low-dose AAV-Cre revealed that single hepatocytes upon YAP activation gradually become smaller and adopt an oval morphology before multiplying and forming large ductular structures (Figure 2A). These clusters costain for YAP, the ductal markers panCK and CK19, and validated progenitor markers, such as SOX9, MIC1C3, and A6 (Figure 2B) (Dorrell et al., 2011; Engelhardt et al., 1993). Furthermore, we noted on a regular basis, that these biliary structures were tightly associated with nontransgenic mesenchyme (Figure S2A). No similar structures were observed in control animals.

To further strengthen these observations, we simultaneously followed the expression of the hepatocyte marker HNF4α and panCK in YAP-expressing clones. These were also lineage traced with a Cre-dependent EYFP reporter (*R26-lsl-EYFP*). As expected, all EYFP+ clones, prior to YAP induction were HNF4α+ and panCK−, confirming the hepatocyte-specific tropism of AAV-Cre (n = 172; Figure 2C). One week after YAP induction, multiple EYFP+ clones (36%, n = 388) could be identified that were double positive for panCK and HNF4α. Interestingly, many of these clones were still composed of single cells, indicating that cell division is not necessary for the initiation of dedifferentiation (Figure 2C). These hybrid cells appeared like neighboring hepatocytes in size and shape, suggesting a transitional state. Moreover, a smaller number of clones had extinguished hepatic gene expression and were solely panCK+ (7%). After Dox administration for 4 weeks, more than 75% of clones were either panCK+ only or contained panCK+/HNF4a+ cells (Figure 2Ci). A complementary quantitative analysis measuring the identity of all transgenic cells, as opposed to clonal output, demonstrates that more than 95% of EYFP+ cells at 4 weeks were panCK+ only (Figure 2Cii). A similar transitional state and clonal fate was observed when costaining for EYFP/HNF4α/SOX9 (Figure S2B). Altogether, our results demonstrate that high levels of YAP are sufficient to impose a ductal/progenitor-like fate on adult hepatocytes in a cell-autonomous manner. These data also highlight that approximately 75% of adult hepatocytes have the capacity to undergo this fate change in vivo.

## Hippo Pathway Signaling Misregulation Results in Hepatocyte Dedifferentiation

We next asked whether changes in endogenous hepatocyte Hippo pathway signaling could lead to hepatocyte dedifferentiation. NF2 is a known potent negative regulator of YAP (Hamaratoglu et al., 2006), and ablation of *Nf2* in all liver cell types results in hepatocellular carcinoma and cholangiocarcinoma (Benhamouche et al., 2010; Zhang et al., 2010). Thus, we surmised that hepatocyte-specific *Nf2* loss would result in liver overgrowth and hepatocyte dedifferentiation into biliary/progenitor cells as observed with our TetOYAP model (Figure 3A). Two months following AAV-Cre administration to $Nf2^{fl/fl}$ mice, we observed ductular structures highly reminiscent of the clusters observed in the TetOYAP model (Figure 3B). Similar to the YAP Tg model, progenitor/ductal structures in the *Nf2* mutant livers stained prominently for YAP, SOX9, and panCK (Figure 3C). Additionally, lineage tracing with an inducible β-galactosidase reporter revealed that such ductular clusters were derived from AAV-Cre-transduced cells (Figure 3B, inset). These data support our hypothesis that changes in endogenous Hippo pathway signaling can reprogram hepatocytes into ductal cells bearing characteristics of hepatic progenitors.

## YAP Expression Activates a Liver Progenitor Cell Program

To understand the molecular basis of YAP-mediated dedifferentiation, and to bring insight into the molecular identity of YAP Tg cells, we isolated EYFP+ cells at multiple time points upon Dox induction and performed FACS purification followed by microarray analysis (Figure 4A). As expected, we observed a widespread and progressive silencing of the hepatocyte phenotype and a gradual acquisition of genes associated with embryonic liver development and ductal/progenitor features (Figures 4B and S3A). Gene set enrichment analysis (GSEA) demonstrates that a gene signature corresponding to endogenous liver progenitors strongly correlated with YAP transgenic cells (Figure S3B). YAP activation does not simply lead to hyperplastic response as no enrichment was found when compared to a gene signature derived from livers recovering from partial hepatectomy (Figure S3C). Our analysis also revealed several upregulated gene programs that define the reprogramming process, including those associated with NOTCH, TGFβ, and EGFR signaling (Figure 4C). This analysis supports the notion that YAP expression in hepatocytes extinguishes hepatocyte-specific gene expression and leads to the specific acquisition of a molecular state resembling endogenous liver progenitors.

## Reintroduction of Hippo Pathway Signaling Induces Differentiated Fates in Reprogrammed Hepatocytes

Our results above suggest that YAP activation in hepatocytes dedifferentiates them into cells that morphologically, phenotypically, and molecularly resemble putative hepatic progenitors. These data support the idea that elevated YAP activity imposes a progenitor state and raises the possibility that reduction of YAP levels in liver progenitors could allow for their differentiation. We thus investigated whether hepatocyte-derived progenitor-like cells obtained after 4 weeks of YAP expression could give rise to mature hepatocytes in situ, following the cessation of Dox administration (Figure 4D).

Corroborating our previous data, 4 weeks post-Dox administration, more than 98% of EYFP+ cells were panCK+ with typical ductal morphology and marked mesenchymal recruitment (Figures 4D and 4E). Following Dox removal (chase period), EYFP+ cells could still be found throughout the liver parenchyma at 4 and 8 weeks (Figure 4E). Although the majority of the EYFP+ cells (~80%) retained a ductal morphology and phenotype, removal of Dox clearly resulted in the emergence of clusters of EYFP+ cells with mature hepatocyte morphology (Figure 4D), which expressed HNF4α but lacked expression of panCK and SOX9 (Figure 4E). Our analysis demonstrates that approximately 20% of EYFP+ cells showed a hepatocyte phenotype following the

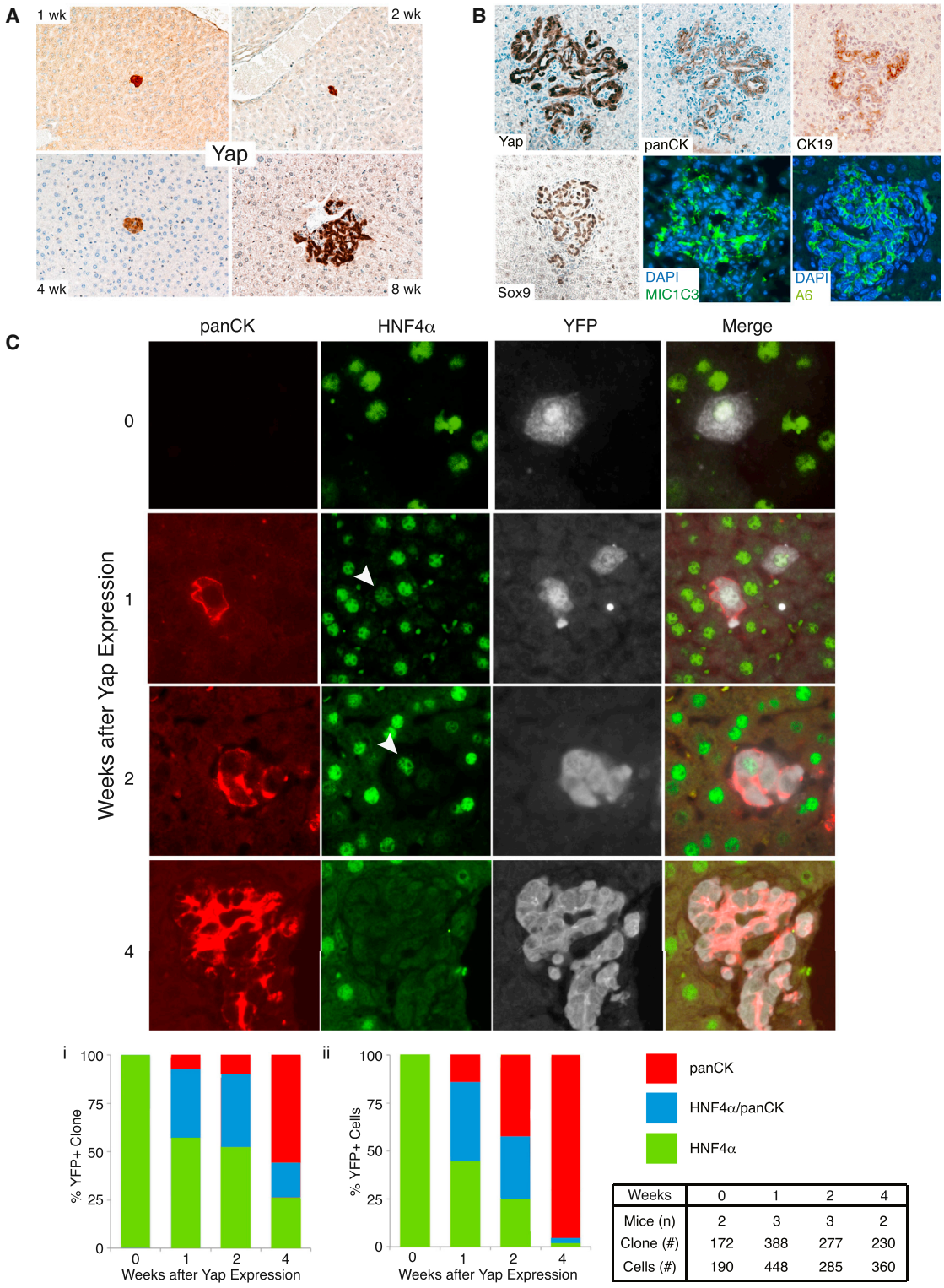


| Weeks | 0 | 1 | 2 | 4 |
|---|---|---|---|---|
| Mice (n) | 2 | 3 | 3 | 2 |
| Clone (#) | 172 | 388 | 277 | 230 |
| Cells (#) | 190 | 448 | 285 | 360 |

**Figure 2. Clonal Analysis of YAP-Mediated Dedifferentiation**

(A) Low-dose ($10^8$ pfu) AAV-Cre and Dox administration allows clonal tracking of hepatocytes expressing YAP for several weeks. Representative images of clonal events at 1, 2, 4, and 8 weeks post-Dox (100×).

(B) Eight weeks post-Dox single hepatocytes give rise to ectopic ductal structures showing expression of multiple progenitor/biliary markers.

*(legend continued on next page)*

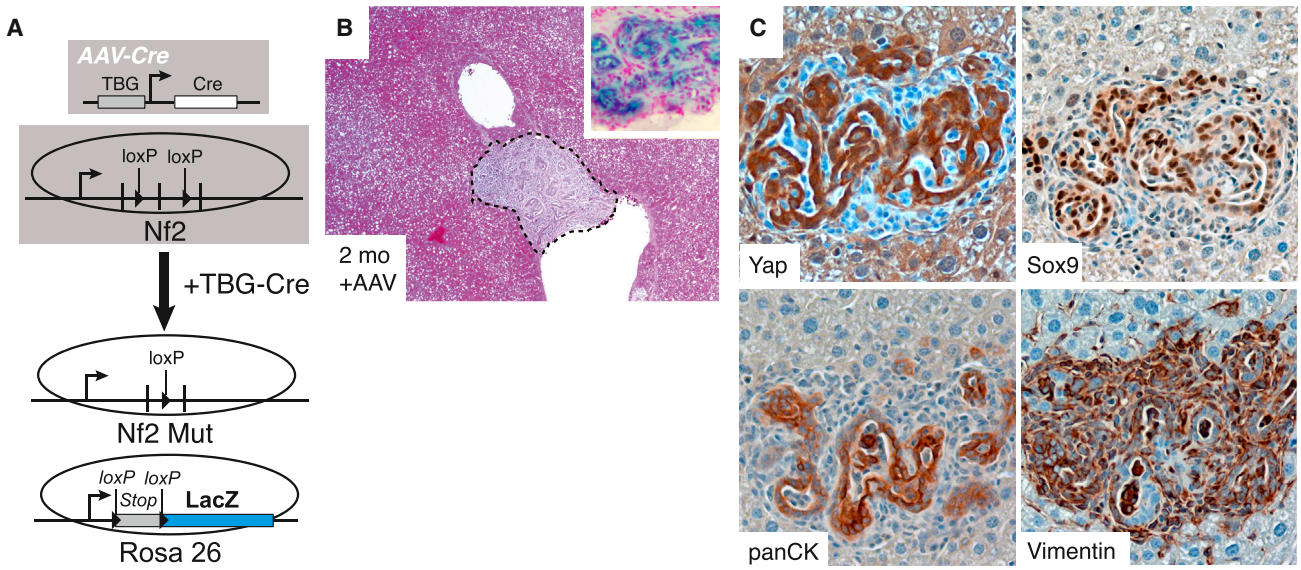


**Figure 3. Hepatocyte-Specific *Nf2* Loss Results in Progenitor/Ductal Dedifferentiation**

(A) Experimental design for generating hepatocyte-specific *Nf2* loss.

(B) Representative H&E stains of *Nf2*-deficient (Mut) livers 2 months after AAV-Cre administration. Inset shows a LacZ-stained nodule from an *Nf2* mutant mouse.

(C) Stained serial section of a biliary malformation for YAP, SOX9, panCK, and Vimentin from an *Nf2* mutant mouse 2 months after AAV-Cre.

chase, compared to only ~1.5% observed in the presence of Dox. Thus, hepatocyte-derived progenitors can redifferentiate into the hepatocyte lineage when normal Hippo pathway signaling is re-established in vivo.

## Hepatocyte-Derived Progenitors Are Clonogenic

To assess progenitor activity in the liver, we utilized a recently developed liver organoid culture system (Figure S4A). Consistent with this report, epithelial organoid structures express ductal progenitor markers but lack hepatocyte gene expression (Figures 5C WT and S4B) (Huch et al., 2013). Interestingly, liver organoids endogenously demonstrate high YAP activity, displaying significant enrichment for a recently described YAP gene signature (Figure S4C) (Mohseni et al., 2014).

We next examined if hepatocyte-derived progenitor-like cells exhibit clonogenic capacity. Whole-dissociated liver cells from AAV-Cre-infected *TetOYAP/R26-lsl-EYFP* mice given Dox for 3 weeks were cultured in organoid media (Figure 5A). Strikingly, hepatocyte-YAP activation results in a striking improvement in organoid number compared with control AAV-infected Dox-uninduced mice (Figure 5B). This effect is also observed when similar epithelial cell numbers are plated (Figure S4D). Importantly, Tg organoids were overwhelmingly EYFP+, indicating their hepatocyte origin, which contrasts with the EYFP−, biliary origin of control organoids (Figures 5B and S1E). Enhancement progenitor output was evident in cultures grown both in the presence and in the absence of Dox (Figures 5B and S4D), demonstrating that organoid identity and growth are independent of expression of the transgene. Hepatocyte-derived organoids displayed immunochemical markers in a similar pattern to WT organoids (Figure 5C). Hierarchical clustering and differential gene expression analysis demonstrated that hepatocyte-derived progenitors are closely related to WT organoids and not to hepatocytes (Figures 5D and 5E). Interestingly, upregulation of fetal hepatoblast markers *Afp* and *Prox1* is observed in hepatocyte-derived, but not in control, organoids (Figure S4F), suggesting potentially that YAP might lead to the activation of an embryonic-like progenitor phenotype. Additionally, hepatocyte-derived organoids are highly enriched for an endogenous liver progenitor gene signature (Figure S4E; $p < 0.001$). In addition, many of the upregulated signaling programs we identified in vivo (Figure 4C) were also found enriched in hepatocyte-derived organoids (Figure S4I).

To conclusively assess the self-renewal, differentiation, and engraftment capacity of hepatocyte-derived progenitors, we generated organoids from single-sorted EYFP+ cells from AAV-Cre/Dox-treated *TetOYAP/R26-lsl-EYFP* mice (Figure 5F). Following single-cell sorting, clonal expansion was carried out in a monolayer, as YAP expression allowed growth and maintenance of the progenitor state in this context (Figures 5G, S4G, and S4H). Addition of a NOTCH inhibitor and Dox withdrawal to these cultures led to suppression of the biliary/progenitor

(C) Clonal and dynamic analysis of fate change driven by YAP. Representative images and quantitation of hepatocyte to progenitor/ductal cell dedifferentiation following YAP expression. Arrowhead indicates weak HNF4α staining. Bar graphs represent measurements of cellular fates as examined by the presence of HNF4α only, HNF4α/panCK, or panCK only in clones or individual cells within clones. Table indicates number of mice, clones, and cells examined for the associated analysis.

See also Figure S2.

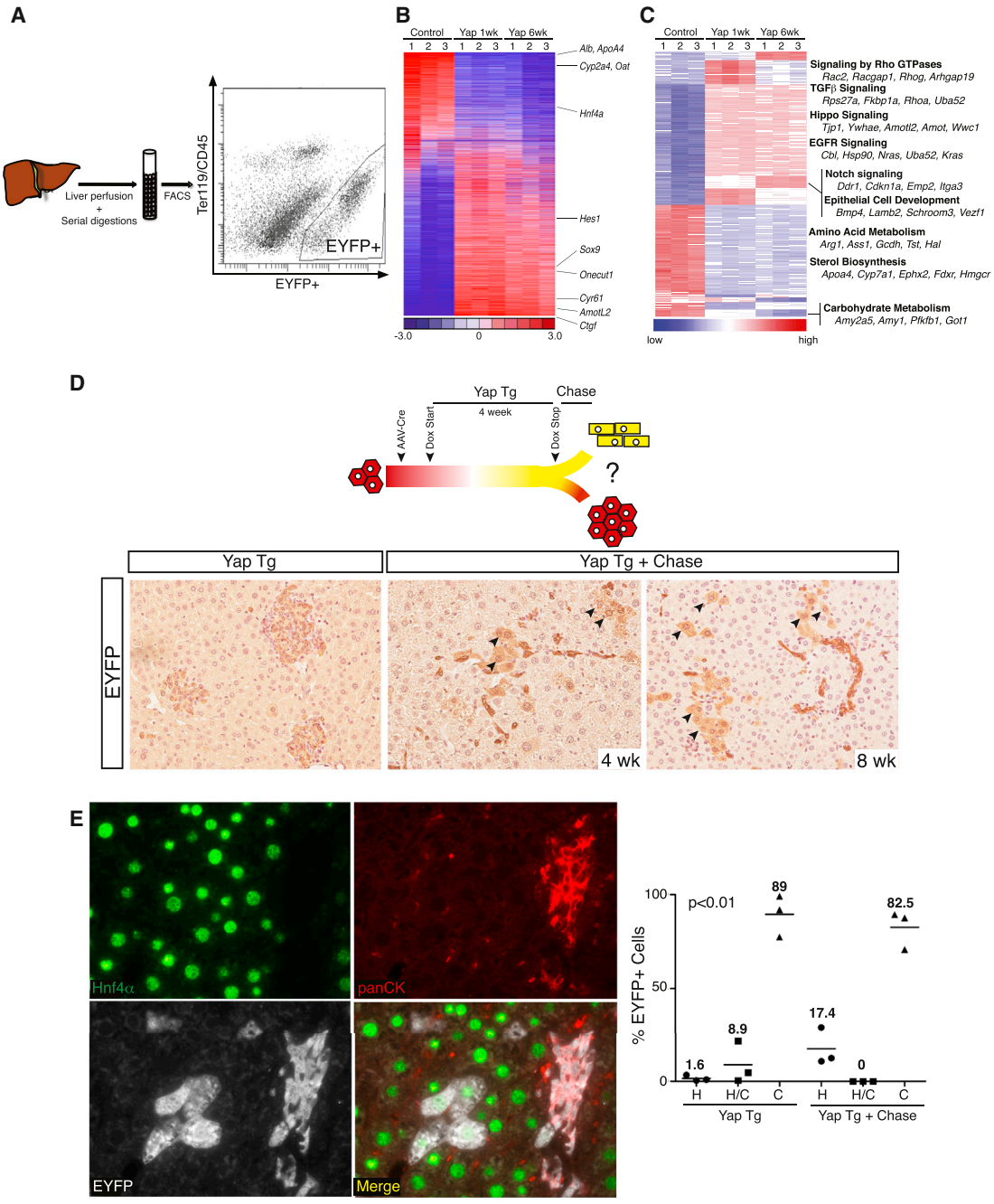


**Figure 4. Molecular Characterization of Dedifferentiated Hepatocytes and Consequences of Restoring Endogenous Hippo Pathway Signaling**

(A) Schematic representation of EYFP+ cell isolation from induced TetOYAP mice. Representative FACS plot 1 week after Dox administration is shown.

(B) Heatmap of 6,536 rank-ordered differentially expressed genes from microarray experiments from hepatocytes (control) and sorted EYFP+ hepatocytes expressing YAP for 1 or 6 weeks. Hepatocytic, biliary, and YAP target genes are indicated to the right.

(C) Heatmap of 1,762 genes grouped by transcriptional gene program using Mclust. Annotated transcriptional programs of interest are noted to the right.

(D) Experimental design for the evaluation of fate outcomes following Dox removal in hepatocytes exposed to Dox for 4 weeks. EYFP stains of representative slides from TetOYAP mice given AAV-cre, placed on Dox for 4 weeks (YAP Tg) and following a 4 or 8 week Dox wash period (YAP Tg + Chase, 200×). Arrowheads indicate EYFP+ cells with hepatocyte morphology.

(E) Triple stain of a representative image (200×) (4 week on, 4 week chase) showing HNF4α (green), panCK (red), EYFP (white), and merge picture. Dot plot of average number of EYFP+ cells for the indicated staining patterns and representative treatments. Horizontal line and number represents the mean. One-way ANOVA was performed using the Kruskal-Wallis test.

See also Figure S3.

fate and emergence of hepatocytic cells (Figure 5H). We next evaluated the in vivo engraftment potential of hepatocyte-derived progenitor clones by transplanting them into fumarylacetoacetate hydrolase-deficient ($Fah^{-/-}$) mice. *Fah* deficiency results in liver failure unless mutant mice are administered 2-[2-nitro-4-(trifluoromethyl)benzoyl]cyclohexane-1,3-dione (NTBC) (Grompe et al., 1995). Differentiated cells derived from a progenitor clone were injected intrasplenically into $Fah^{-/-}$ mice (Figure 5F), and 4–5 months posttransplantation donor cell engraftment was assessed by IHC. Remarkably, three out of four recipient mice displayed evidence of widespread repopulation (>60%) by EYFP+ cells (Figure 5I). $EYFP^{+}$ clusters stained positive for FAH and HNF4α and negative for CK19 (Figure 5I), indicating an acquisition of a mature hepatocyte phenotype. Our results are similar to the extent of repopulation typically observed upon transplantation of freshly isolated hepatocytes (Figure S4J). These results highlight the capacity of hepatocyte-derived progenitors to be amplified and to undergo redifferentiation into hepatocytes at the single-cell level. Overall, our data suggest that YAP activation in mature hepatocytes is sufficient for imposing a molecular and bona fide functional progenitor state.

## NOTCH Signaling Downstream of YAP during Reprogramming

In our bioinformatic analysis of pathways activated in response to hepatocyte-specific YAP expression, we found several upregulated developmental cascades that could explain some of the phenotypes observed (Figures 4C and S4I). The most upregulated pathway in vivo and in vitro was NOTCH signaling. This pathway is known to be an important determinant of biliary cell fate and growth during embryogenesis (Hofmann et al., 2010; Zong et al., 2009). Quantitative real-time PCR of EYFP+-sorted cells 1 week after YAP activation confirmed striking upregulation of several members of the NOTCH pathway, including *Notch1/2*, *Jag1*, and the NOTCH target genes *Hes1* and *Sox9* (Figure 6A). Immunostaining for HES1 confirmed NOTCH pathway activation in YAP-expressing hepatocytes (Figure 6B). We next investigated whether some of these NOTCH genes are direct transcriptional targets of the YAP/TEAD complex. Analysis of published genome-wide chromatin occupancy revealed significant enrichment of TEAD4 in the promoter regions of *Notch2* and *Sox9* in mouse trophoblast stem cells (Home et al., 2012). We validated the presence of TEAD4 binding in these regions using chromatin immunoprecipitation (ChIP) in dedifferentiated hepatocytes and also demonstrated robust binding of YAP (Figure 6C). Furthermore, analysis of human ChiP-Seq data for TEAD4 in human HepG2 cells exposed conserved regions of occupancy in both *NOTCH2* and *SOX9* (Figure S5A). TEAD4 and YAP binding in these regions was confirmed by ChIP-PCR (Figure S5A). We focused on the bound region of *Notch2* as YAP/TEAD binding to this region displayed the highest signal-to-noise ratio. Additionally, NOTCH2 is the critical mammalian NOTCH receptor involved in ductal development (Geisler et al., 2008; McCright et al., 2002). We found two TEAD consensus binding sites in a region 750–1,150 bp downstream of the *Notch2* transcriptional start site. This region was cloned into a luciferase reporter plasmid to evaluate its responsiveness to YAP/TEAD. Expression of YAPS127A drastically increased luciferase activity in cholangiocarcinoma cells, whereas YAPS94A, a YAP mutant unable to bind TEAD proteins (Zhao et al., 2008), had no effect on reporter activity. As predicted, mutation of the TEAD binding sites in the *Notch2* promoter region abrogates the YAPS127A-driven increase in luciferase expression (Figure 6D), indicating a functional role for these elements in driving *Notch2* gene expression. In support of YAP being important for the expression of *Notch2*, Ad-Cre-mediated deletion of *Yap* and its homolog *Taz* in liver organoids derived from $Yap^{fl/fl}/Taz^{fl/fl}$ conditional knockout mice results in an acute and significant downregulation of *Notch2* transcript levels (Figure 6E). Similarly, YAP/TAZ knockdown in human cholangiocarcinoma cells results in 50%–75% reduction of *Notch2* mRNA (Figure S5B). Thus, our results suggest that YAP/TEAD directly regulates transcription of *Notch2* and other NOTCH pathway genes to modulate NOTCH signaling.

Finally, we sought to examine the functional role of NOTCH signaling downstream of YAP in vivo. Despite the many NOTCH receptors, NOTCH signaling is mediated through a single transcriptional coactivator, RBPJ. We generated *TetOYAP* mice also carrying a conditional *Rpbj* and *mT/mG* reporter alleles (Figure 7A), which were then treated with AAV-Cre followed by Dox treatment. Control experiments demonstrated high-efficiency *Rbpj* deletion exclusively in the hepatocytic compartment of injected mice (Figure S6B). At high doses of AAV-Cre, deletion of *Rbpj* dampened the appearance of small ductal-looking cells and overall liver hyperplasia (Figure S6A), and significantly reduced the number of CK19- and JAG1-positive cells emerging 2 weeks following Dox treatment (Figure 7B). *Ck19* and *Jag1* are not considered RPBJ transcriptional targets. Even more striking observations were made in the low-dose context, where clonal outputs could be measured and evaluated at longer time points. These experiments demonstrate that NOTCH inhibition resulted in a significant and drastic reduction in the size of dedifferentiated clones (Figure 7C). Additionally, the vast majority of *Rbpj*-mutant clusters exhibited poorly developed biliary morphology and absent mesenchymal recruitment (Figures 7C and 7D). Clonal analyses revealed that fate outputs of YAP-expressing hepatocytes were altered in the absence of NOTCH signaling, as only 25% of clones were CK19+/HNF4α− compared to >97% of control clones at 12 weeks of induction (Figure 7D). Single transcript in situ hybridization confirmed reduction of mRNA in *Rbpj* mutant clones (Figure S6C). Altogether, these data provide evidence that Hippo/YAP act upstream of the NOTCH-signaling pathway, whose activity is important for hepatocyte-to-ductal dedifferentiation and clonal outgrowth.

## DISCUSSION

The fate relationship among hepatocytes, ductal cholangiocytes, and putative liver progenitors is a matter of debate (Greenbaum, 2011; Michalopoulos, 2012). Whereas lineage tracing data support the idea of a ductal progenitor-like cells giving rise to hepatocytes (Furuyama et al., 2010; Huch et al., 2013), there is also evidence that hepatocytes might give rise to cells of the ductal lineage. For instance, periportal hepatocytes in patients with cholestatic or biliary autoimmune disorders can

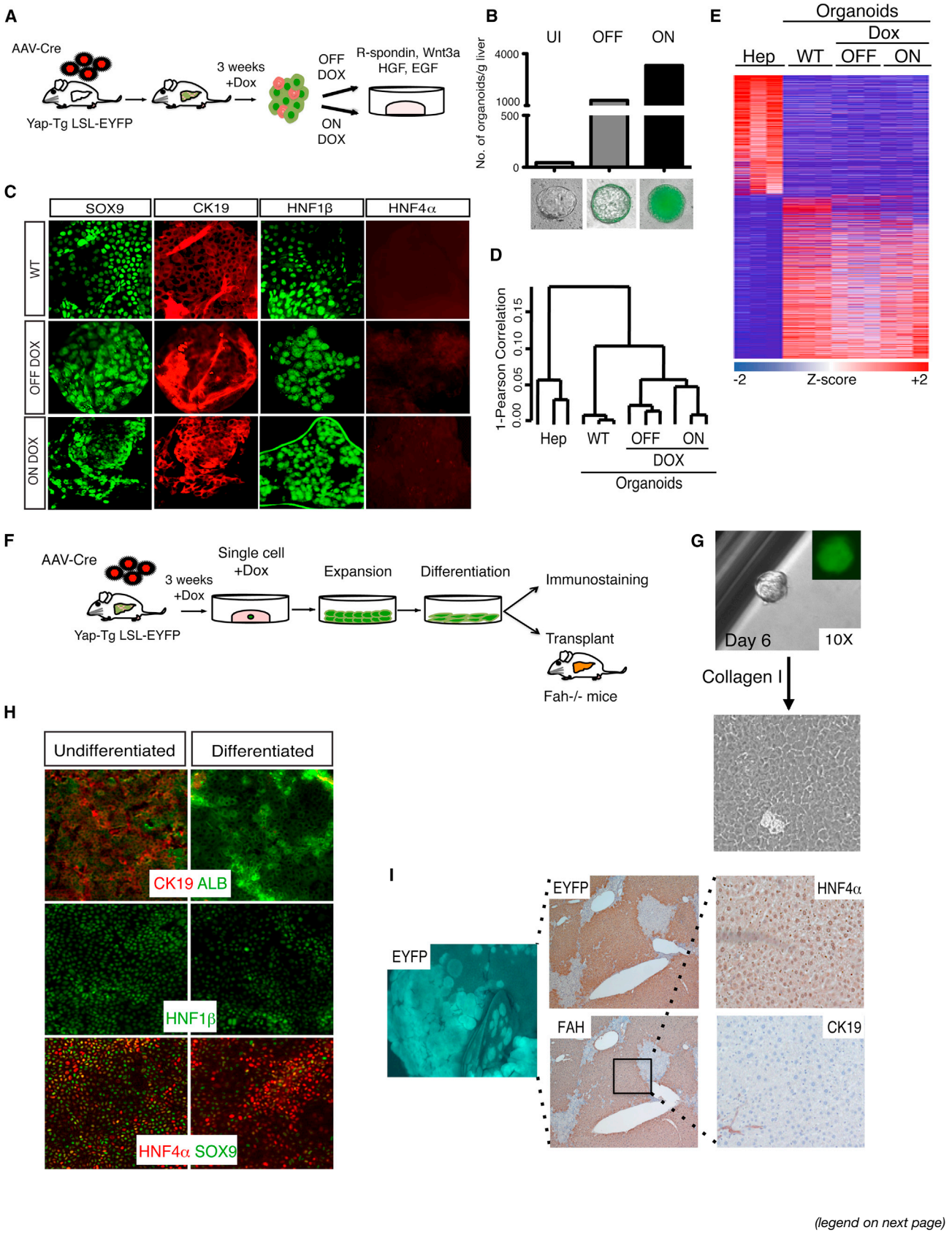


*(legend on next page)*

express biliary-specific markers (Gouw et al., 2011). Additionally, hepatocyte transplantation in the rat supports the possibility of hepatocyte "transdifferentiation" into ductal cells (Michalopoulos et al., 2005). More recently, lineage-tracing experiments using AAV-Cre have demonstrated the capacity of adult hepatocytes to give rise to cells with morphological and molecular features of biliary epithelial cells during injury (Yanger et al., 2013). However, Malato et al. (2011) failed to observe hepatocyte-derived contribution in a similar animal model. Other findings have shown that dual NOTCH and AKT signaling in hepatocytes can lead to their conversion into biliary cells that eventually progress into cholangiocarcinomas, a malignancy typically associated with a ductal origin (Fan et al., 2012; Komuta et al., 2012). Our work here provides definitive evidence that adult hepatocytes have the potential to not only give rise to cells with ductal characteristics but also cells that molecularly and functionally resemble liver progenitors or "oval" cells. The observation that a large proportion of hepatocytes (~75%) undergo dedifferentiation suggests that most hepatocytes intrinsically harbor this developmental capacity. Thus, our studies raise the possibility that hepatocytes are inherently plastic and might participate in liver repair not only by self-duplication but also by dedifferentiation into progenitor cells.

Our work reveals a unique role for Hippo/YAP signaling in liver biology. The observed differential transcriptional output of YAP between hepatocytes and progenitor cells suggests that different YAP levels/activity could determine different hepatic cell fates. Perhaps intermediate YAP levels would then specify a differentiated ductal cell or cholangiocyte fate. This idea is supported by the finding of cholangiocyte hypoplasia in mice with a developmental deletion of YAP in the liver (Zhang et al., 2010). In this regard, it will be interesting to determine the mechanisms that allow for robust YAP activation in a small subset of biliary cells. Our data also show that NF2 is an important endogenous regulator of YAP in hepatocytes. Previous work using a developmental deletion of *Nf2* in all liver cells demonstrated the outgrowth of ductular cells and eventual development of cholangiocarcinoma (Benhamouche et al., 2010; Zhang et al., 2010). These findings were interpreted as oval-cell expansion and transformation driven by loss of Hippo signaling. Our findings, alternatively, suggest that hepatocytes are the source of this ductular outgrowth. Combined with recent findings (Fan et al., 2012; Sekiya and Suzuki, 2012; Zender et al., 2013), our work argues in favor of a paradigm in which hepatocytes might be the cell-of-origin not only for cholangiocarcinoma but also for mixed-phenotype liver cancer, typically thought to arise from oval cells.

Little is known about the identity of functional targets that act downstream of YAP. NOTCH signaling has been shown to be important for ductal specification during development (Hofmann et al., 2010; Zong et al., 2009) and is also transiently activated during liver regeneration (Köhler et al., 2004). Our data demonstrate that YAP/TEAD can directly control the expression of the NOTCH2 receptor, likely regulating signaling. YAP/TEAD also regulate *Sox9* expression, itself a NOTCH target, suggesting that YAP simply does not act upstream of NOTCH but that multiple layers of signaling crosstalk exist during progenitor/ductal specification. Our clonal epistatic analysis using *Rbpj*-deficient mice provides evidence indicating that NOTCH signaling is important downstream of YAP for the outgrowth of YAP-driven clones. NOTCH is also important, though not essential, for some aspects of the fate-switching phenotype, such as upregulation of cytokeratins and mesenchymal recruitment. NOTCH is not required for the upregulation of other ductal/progenitor markers, such as SOX9 and osteopontin (data not shown), suggesting participation of other molecules downstream of YAP. It has also been suggested that JAG1 can be a target of YAP in hepatocellular carcinoma (Tschaharganeh et al., 2013). Although other mechanisms downstream of YAP are likely at play, our experiments suggest that YAP-driven tumors might benefit from treatment with NOTCH inhibitors.

Our results demonstrate that tissue-specific progenitor cells can be obtained from genetic manipulation of a mature cell type in vivo. The extremely high efficiency and the rapid kinetics of the dedifferentiation process suggest that this manipulation might be used as a therapeutic strategy for inducing liver repair. Transient inhibition of the Hippo kinases could be pursued to do this. Because hepatocytes are relatively abundant, it is also conceivable that these cells could be used for the generation of progenitors cells ex vivo. Additionally, YAP activation confers increased proliferative capacity and allows for monolayer growth of progenitors initially grown in organoid-like cultures, facilitating their maintenance, expandability in culture, and potential clinical application. Together, our work lays the groundwork for the

**Figure 5. YAP-Reprogrammed Progenitors Are Clonogenic and Produce Hepatocyte Progeny**

(A) Schematic representation of liver organoid generation from YAP Tg mice and expansion procedure.

(B) Analysis of the number of organoids derived from livers from AAV-Cre-infected Dox-uninduced (UI) and 3-week-induced YAP Tg mice. YAP Tg results in dramatic increase of the liver organoid generation, both in the presence (ON) and in the absence (OFF) of Dox in culture. Bottom shows representative immunofluorescent (IF) images of organoids in each category. Bars represent value of n = 3.

(C) IF of wild-type (WT), ON Dox YAP Tg, and OFF Dox YAP Tg organoids for biliary (SOX9, CK19, HNF1β) and hepatocyte (HNF4α) markers.

(D) Hierarchical clustering analysis of primary hepatocytes, WT, and hepatocyte-derived YAP Tg organoids demonstrates close clustering of all organoid groups.

(E) Differential expression analysis of hepatocytes compared to distinct organoid populations. Heatmap demonstrates all differentially expressed genes with ≥2.5 fold change.

(F) Experimental design for the isolation, expansion, and characterization of single-cell hepatocyte-derived organoids.

(G) Representative image of organoid derived from single-sorted EYFP+ YAP Tg cell, followed by monolayer expansion.

(H) Differentiation of hepatocyte-derived organoid clone in the presence of γ-secretase inhibitor and in the absence of Dox. Day 15 differentiated cells demonstrate downregulation of biliary (CK19, SOX9, HNF1β) and increase of hepatocyte markers (ALB, HNF4α).

(I) Representative liver images 5 months after transplantation of differentiated clonal YAP-Tg cells into $Fah^{-/-}$ mice. Engrafted cells are positive for EYFP (5x), FAH (5x), and HNF4α (hepatocyte marker) and negative for CK19 (biliary marker).

See also Figure S4.

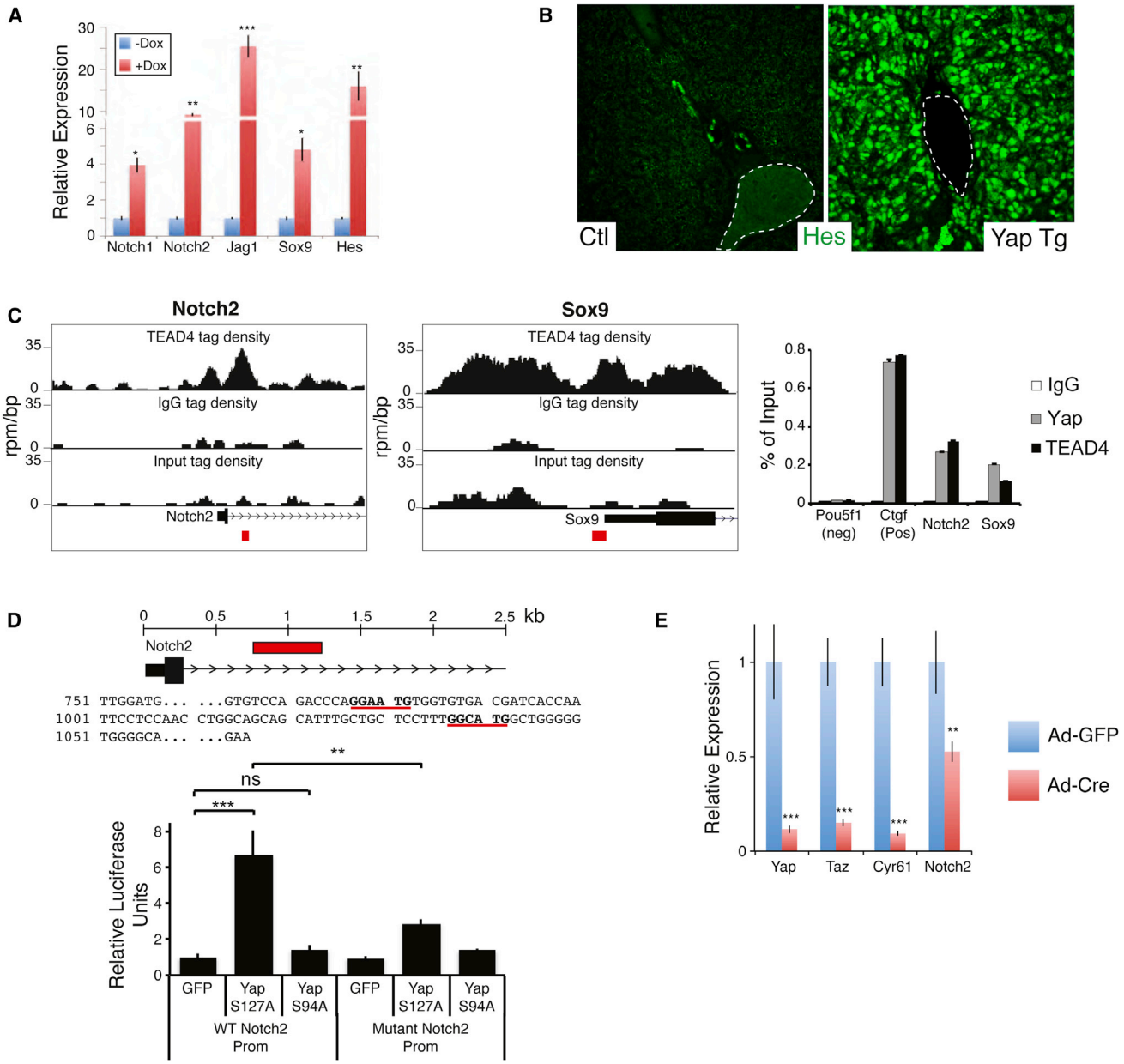


**Figure 6. YAP and TEAD Regulate *Notch2* Transcription**

(A) Quantitative real-time PCR analysis of NOTCH pathway genes from EYFP+-sorted uninduced and 1 week Dox YAP Tg liver cells post-AAV-Cre infection. n = 3, mean ± SEM.

(B) Immunofluorescent analysis for HES1 in an uninduced (Ctl) and a 2 week YAP Tg mouse. Dotted line outlines portal vein.

(C) ChIP-Seq binding profiles (reads per million per base pair) for TEAD4 at the *Notch2* and *Sox9* loci in trophoblast stem cells. Graph on the right shows ChIP-PCR assays for the indicated validation sites (red boxes) performed in liver cells isolated from YAP Tg mice 2 weeks post-Dox. Graph on the right shows a representative ChIP-PCR assay for the indicated validation sites (red boxes) performed in liver cells isolated from Yap Tg mice 2 weeks post-Dox. Mean ± SEM.

(D) Localization and sequence of TEAD binding sites (bold and underlined) present in the *NOTCH2* promoter. Red box indicates area of genomic sequence (WT *Notch2* prom) that was cloned into a luciferase expression construct for functional analyses in CCLP1 cells (bottom). Mutant *Notch2* promoter construct contains three mutated base pairs at each of the TEAD binding sites. n = 3, mean ± SEM.

(E) Quantitative real-time PCR analysis of the indicated target genes in $Yap^{fl/fl}$ $Taz^{fl/fl}$ liver organoids given either Adenovirus-EGFP or Ad-Cre:EGFP. mRNA analysis of sorted infected cells was done 48 hr following infection. n = 3, mean ± SD. *p < 0.05; **p < 0.01; ***p < 0.001.

See also Figure S5.

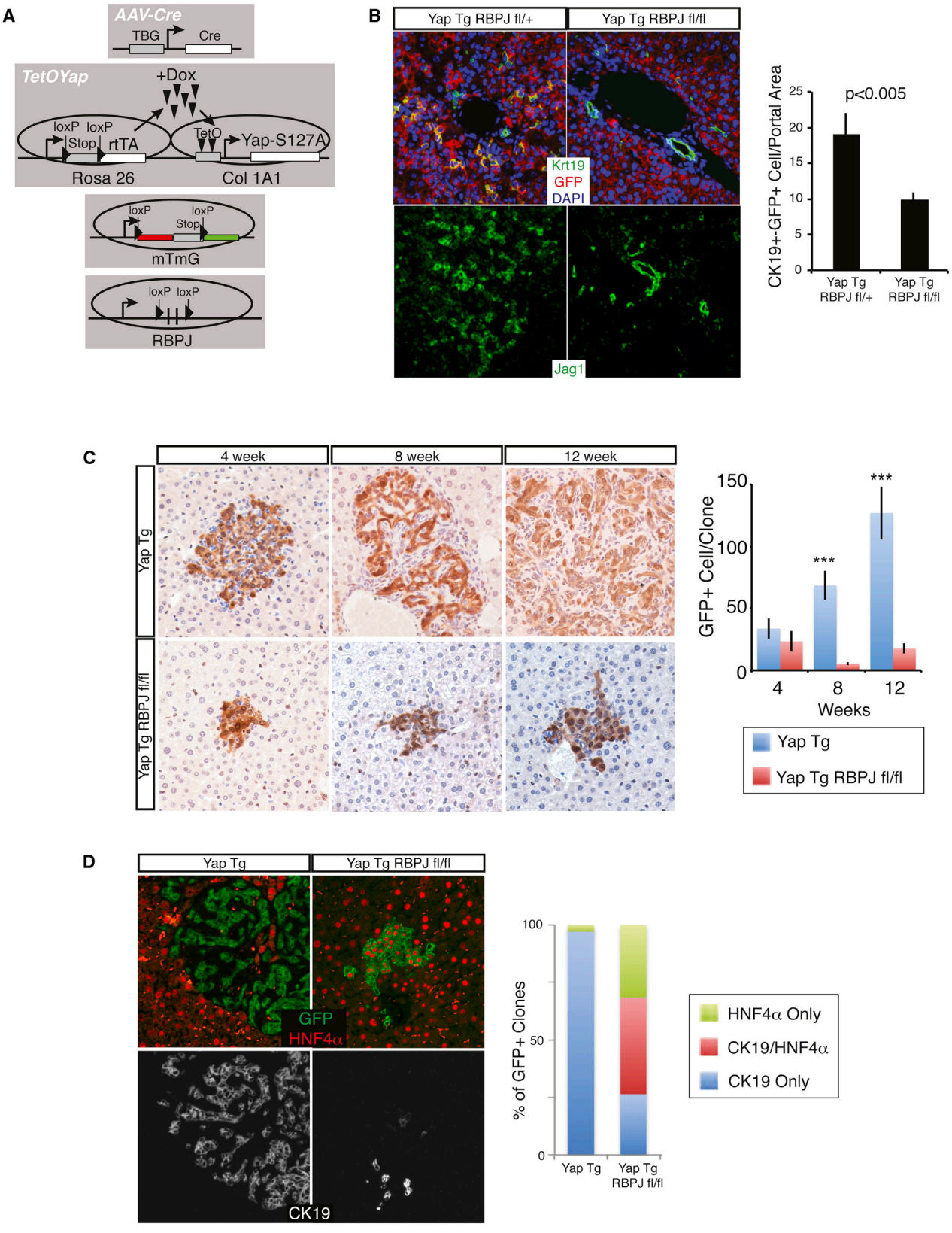


*(legend on next page)*

manipulation of Hippo pathway signaling for regenerative medicine of liver disease. More broadly, our experiments suggest that adult-differentiated epithelial cells could be manipulated for the generation of tissue-specific progenitor or stem cells.

## EXPERIMENTAL PROCEDURES

Full details are provided in the Extended Experimental Procedures.

### Mouse Lines, AAV Virus Administration, Tamoxifen Induction, and YAP Overexpression

FRG-NOD (Yecuris), tetracycline-inducible YAP expression (Camargo et al., 2007), *Ck19-CreERT2* (Means et al., 2008), conditional *Rbpj* (Han et al., 2002), and *Nf2* (Benhamouche et al., 2010) deletion mice are utilized in this study. *Ctgf-EGFP* mice were derived from GENSAT. Male and female mice were used in this study (except for microarray analysis) and did not show sex-bias differences. AAV-TBG cre (University of Pennsylvania Vector Core, AV-8-PV1091) was given to 4- to 8-week-old mice retro-orbitally. After 3 days, mice were administered doxycycline (1 mg/ml) ad libitum in their cage water. For Ck19-CreERT mice, 4- to 8-week-old mice were given 3 mg of tamoxifen for 5 sequential days. Two weeks later, doxycycline was started. A minimum of three mice was examined per experiment. Conditional Rosa26 β-galactosidase, EYFP, and mT/mG mice were obtained from Jackson Laboratory. All mouse procedures and protocols were approved by an AAALAC-accredited facility.

### Liver Organoid Growth Medium

Cultures were performed as described with slight modifications (Huch et al., 2013). Liver organoid medium consists of Dulbecco's modified Eagle's medium /F12 medium (Invitrogen), 1× N2-supplement (Invitrogen), 1× B27 without vitamin A-supplement (Invitrogen), 10 mM nicotinamide (Sigma-Aldrich), 0.001 mM dexamethasone (Sigma-Aldrich), 10 mM HEPES (Invitrogen), and 20 μM Y27632 (Sigma-Aldrich). rmEGF (50 ng/ml; R&D Systems), rmHGF (40 ng/ml; Peprotech), rmWnt3a (100 ng/ml; Peprotech), and rhRspo1 (500 ng/ml; R&D) were used as growth factor supplements. Growth factors were replaced every other day, whereas fresh media was added every 4 days.

### Liver Organoid Generation

Isolated livers from newborn or adult mice were mechanically diced and digested. Filtered and pelleted cells were resuspended in ice-cold growth-factor-reduced matrigel (BD Biosciences) with the growth factor cocktail. Polymerization of cell/matrigel mixture was performed at 37°C for 30 min, followed by the addition of liver organoid growth medium. Liver organoid colonies were observed at 7–10 days upon initial cell plating. To generate organoids from YAP Tg mice, YAP was induced for 3 weeks in the TetOYAP line, and organoids were generated in ± Dox conditions.

### Luciferase Assay

The indicated portion of the Notch2 promoter construct cloned into the pGL3-Basic vector (Promega). At the two TEA binding sites identified within the Notch2 promoter, three point mutations were generated at each site, and this fragment was also cloned into the same vector. CCLP1 cells were cotransfected with a Renilla plasmid and the constructs of interest. Cells were harvested 72 hr later using the Dual-Glo Luciferase Assay System (Promega) and assayed in accordance with the manufacturer's directions.

## ACCESSION NUMBERS

The Gene Expression Omnibus accession number for the gene arrays reported in this paper is GSE55560.

## SUPPLEMENTAL INFORMATION

Supplemental Information includes Extended Experimental Procedures, six figures, and four tables and can be found with this article online at http://dx.doi.org/10.1016/j.cell.2014.03.060.

## AUTHOR CONTRIBUTIONS

D.Y. and F.D.C. designed experiments relevant to the hepatocyte-specific YAP expression. C.C. and F.D.C. designed experiments relevant to organoid cultures. D.Y., C.C., and F.D.C. wrote the manuscript. D.Y., C.C., G.G.G., B.G., K.S., B.P.-M., K.Y., and B.Z.S. performed experiments and data analysis. P.C. performed bioinformatic analysis. F.D.C. supervised the project and gave final approval.

## ACKNOWLEDGMENTS

We are grateful for stimulating discussions with the Camargo lab members, Barbara Trejo for help with IHC, Roderick Bronson for reviewing mouse liver pathology, and Ron Mathieu of the Stem Cell Program FACS facility. We thank G. Gu, T. Honjo, and M. Giovannini for use of *Ck19-CreERT*, *RPBJ*, and *Nf2* mice, respectively. V. Factor generously donated A6 antibody for our use. This study was supported by awards from the Stand Up to Cancer-AACR initiative (FDC), grants from the National Institutes of Health (AR064036 and DK099559 to F.D.C.; DK083355 to B.Z.S.), a Department of Defense award (W81XWH-9) (to F.D.C.), and Junior Investigator funds from the Harvard Stem Cell Institute (to F.D.C.). D.Y. is supported by the National Institute of Diabetes and Digestive and Kidney Diseases (5T32 DK007477-27) and a Boston Children's Hospital Career Development Award and is a George Ferry Young Investigator (NASPGHAN). G.G.G. is supported by an American-Italian Cancer Foundation postdoctoral research fellowship. B.P.-M. is supported by the National Science Foundation Graduate Research Fellowship Program (DGE1144152). F.D.C. is a Pew Scholar in the Biomedical Sciences.

Received: July 3, 2013
Revised: February 4, 2014
Accepted: March 19, 2014
Published: June 5, 2014

## REFERENCES

Benhamouche, S., Curto, M., Saotome, I., Gladden, A.B., Liu, C.-H., Giovannini, M., and McClatchey, A.I. (2010). Nf2/Merlin controls progenitor homeostasis and tumorigenesis in the liver. Genes Dev. *24*, 1718–1730.

Camargo, F.D., Gokhale, S., Johnnidis, J.B., Fu, D., Bell, G.W., Jaenisch, R., and Brummelkamp, T.R. (2007). YAP1 increases organ size and expands undifferentiated progenitor cells. Curr. Biol. *17*, 2054–2060.

Demetris, A.J., Seaberg, E.C., Wennerberg, A., Ionellie, J., and Michalopoulos, G. (1996). Ductular reaction after submassive necrosis in humans. Special emphasis on analysis of ductular hepatocytes. Am. J. Pathol. *149*, 439–448.

**Figure 7. NOTCH Signaling Is a Functional Target of YAP/TEAD In Vivo**

(A) Experimental design for hepatocyte-specific YAP overexpression with concomitant loss of NOTCH signaling.

(B) CK19 (green), GFP (red), and DAPI (blue) or JAG1 immunofluorescence (IF) in *TetOYAP:Rbpj*$^{fl/+}$ and *TetOYAP:Rbpj*$^{fl/fl}$ mice infected with high-dose AAV-Cre and treated with Dox for 2 weeks. Bar graph shows quantitation of GFP+CK19+ cells. n = 3, mean ± SEM.

(C) GFP stain of representative animals infected with low-dose AAV-Cre and treated with Dox for the indicated times. Graph on the right depicts the number of GFP+ cells per clone analyzed. n = 3, mean ± SEM.

(D) Representative IF triple stain (GFP, HNF4α, CK19) of single-cell-derived clones with the noted genotypes, 12 weeks after Dox induction. Bar graph represents proportion of clones displaying indicated markers. ***$p < 0.001$.

See also Figure S6.

Dong, J., Feldmann, G., Huang, J., Wu, S., Zhang, N., Comerford, S.A., Gayyed, M.F., Anders, R.A., Maitra, A., and Pan, D. (2007). Elucidation of a universal size-control mechanism in Drosophila and mammals. Cell *130*, 1120–1133.

Dorrell, C., Erker, L., Schug, J., Kopp, J.L., Canaday, P.S., Fox, A.J., Smirnova, O., Duncan, A.W., Finegold, M.J., Sander, M., et al. (2011). Prospective isolation of a bipotential clonogenic liver progenitor cell in adult mice. Genes Dev. *25*, 1193–1203.

Engelhardt, N.V., Factor, V.M., Medvinsky, A.L., Baranov, V.N., Lazareva, M.N., and Poltoranina, V.S. (1993). Common antigen of oval and biliary epithelial cells (A6) is a differentiation marker of epithelial and erythroid cell lineages in early development of the mouse. Differentiation *55*, 19–26.

Espanol-Suner, R., Carpentier, R., Van Hul, N., Legry, V., Achouri, Y., Cordi, S., Jacquemin, P., Lemaigre, F., and Leclercq, I.A. (2012). Liver progenitor cells yield functional hepatocytes in response to chronic liver injury in mice. Gastroenterology *143*, 1564–1575.e7.

Fan, B., Malato, Y., Calvisi, D.F., Naqvi, S., Razumilava, N., Ribback, S., Gores, G.J., Dombrowski, F., Evert, M., Chen, X., and Willenbring, H. (2012). Cholangiocarcinomas can originate from hepatocytes in mice. J. Clin. Invest. *122*, 2911–2915.

Furuyama, K., Kawaguchi, Y., Akiyama, H., Horiguchi, M., Kodama, S., Kuhara, T., Hosokawa, S., Elbahrawy, A., Soeda, T., Koizumi, M., et al. (2010). Continuous cell supply from a Sox9-expressing progenitor zone in adult liver, exocrine pancreas and intestine. Nat. Genet. *43*, 34–41.

Geisler, F., Nagl, F., Mazur, P.K., Lee, M., Zimber-Strobl, U., Strobl, L.J., Radtke, F., Schmid, R.M., and Siveke, J.T. (2008). Liver-specific inactivation of Notch2, but not Notch1, compromises intrahepatic bile duct development in mice. Hepatology *48*, 607–616.

Gouw, A.S., Clouston, A.D., and Theise, N.D. (2011). Ductular reactions in human liver: diversity at the interface. Hepatology *54*, 1853–1863.

Greenbaum, L.E. (2011). The ductal plate: a source of progenitors and hepatocytes in the adult liver. Gastroenterology *141*, 1152–1155.

Grompe, M., Lindstedt, S., al-Dhalimy, M., Kennaway, N.G., Papaconstantinou, J., Torres-Ramos, C.A., Ou, C.N., and Finegold, M. (1995). Pharmacological correction of neonatal lethal hepatic dysfunction in a murine model of hereditary tyrosinaemia type I. Nat. Genet. *10*, 453–460.

Hamaratoglu, F., Willecke, M., Kango-Singh, M., Nolo, R., Hyun, E., Tao, C., Jafar-Nejad, H., and Halder, G. (2006). The tumour-suppressor genes NF2/Merlin and Expanded act through Hippo signalling to regulate cell proliferation and apoptosis. Nat. Cell Biol. *8*, 27–36.

Han, H., Tanigaki, K., Yamamoto, N., Kuroda, K., Yoshimoto, M., Nakahata, T., Ikuta, K., and Honjo, T. (2002). Inducible gene knockout of transcription factor recombination signal binding protein-J reveals its essential role in T versus B lineage decision. Int. Immunol. *14*, 637–645.

Hofmann, J.J., Zovein, A.C., Koh, H., Radtke, F., Weinmaster, G., and Iruela-Arispe, M.L. (2010). Jagged1 in the portal vein mesenchyme regulates intrahepatic bile duct development: insights into Alagille syndrome. Development *137*, 4061–4072.

Home, P., Saha, B., Ray, S., Dutta, D., Gunewardena, S., Yoo, B., Pal, A., Vivian, J.L., Larson, M., Petroff, M., et al. (2012). Altered subcellular localization of transcription factor TEAD4 regulates first mammalian cell lineage commitment. Proc. Natl. Acad. Sci. USA *109*, 7362–7367.

Huch, M., Dorrell, C., Boj, S.F., van Es, J.H., Li, V.S., van de Wetering, M., Sato, T., Hamer, K., Sasaki, N., Finegold, M.J., et al. (2013). In vitro expansion of single Lgr5+ liver stem cells induced by Wnt-driven regeneration. Nature *494*, 247–250.

Köhler, C., Bell, A.W., Bowen, W.C., Monga, S.P., Fleig, W., and Michalopoulos, G.K. (2004). Expression of Notch-1 and its ligand Jagged-1 in rat liver during liver regeneration. Hepatology *39*, 1056–1065.

Komuta, M., Govaere, O., Vandecaveye, V., Akiba, J., Van Steenbergen, W., Verslype, C., Laleman, W., Pirenne, J., Aerts, R., Yano, H., et al. (2012). Histological diversity in cholangiocellular carcinoma reflects the different cholangiocyte phenotypes. Hepatology *55*, 1876–1888.

Lee, K.-P., Lee, J.-H., Kim, T.-S., Kim, T.-H., Park, H.-D., Byun, J.-S., Kim, M.-C., Jeong, W.-I., Calvisi, D.F., Kim, J.-M., and Lim, D.S. (2010). The Hippo-Salvador pathway restrains hepatic oval cell proliferation, liver size, and liver tumorigenesis. Proc. Natl. Acad. Sci. USA *107*, 8248–8253.

Li, H., Wolfe, A., Septer, S., Edwards, G., Zhong, X., Bashar Abdulkarim, A., Ranganathan, S., and Apte, U. (2011). Deregulation of Hippo kinase signalling in human hepatic malignancies. Liver Int. *32*, 38–47.

Lu, L., Li, Y., Kim, S.M., Bossuyt, W., Liu, P., Qiu, Q., Wang, Y., Halder, G., Finegold, M.J., Lee, J.-S., and Johnson, R.L. (2010). Hippo signaling is a potent in vivo growth and tumor suppressor pathway in the mammalian liver. Proc. Natl. Acad. Sci. USA *107*, 1437–1442.

Malato, Y., Naqvi, S., Schürmann, N., Ng, R., Wang, B., Zape, J., Kay, M.A., Grimm, D., and Willenbring, H. (2011). Fate tracing of mature hepatocytes in mouse liver homeostasis and regeneration. J. Clin. Invest. *121*, 4850–4860.

McCright, B., Lozier, J., and Gridley, T. (2002). A mouse model of Alagille syndrome: Notch2 as a genetic modifier of Jag1 haploinsufficiency. Development *129*, 1075–1082.

Means, A.L., Xu, Y., Zhao, A., Ray, K.C., and Gu, G. (2008). A CK19(CreERT) knockin mouse line allows for conditional DNA recombination in epithelial cells in multiple endodermal organs. Genesis *46*, 318–323.

Michalopoulos, G.K. (2012). Phenotypic fidelity (or not?) of epithelial cells in the liver. Hepatology *55*, 2024–2027.

Michalopoulos, G.K., Barua, L., and Bowen, W.C. (2005). Transdifferentiation of rat hepatocytes into biliary cells after bile duct ligation and toxic biliary injury. Hepatology *41*, 535–544.

Mohseni, M., Sun, J., Lau, A., Curtis, S., Goldsmith, J., Fox, V.L., Wei, C., Frazier, M., Samson, O., Wong, K.K., et al. (2014). A genetic screen identifies an LKB1-MARK signalling axis controlling the Hippo-YAP pathway. Nat. Cell Biol. *16*, 108–117.

Oertel, M., and Shafritz, D. (2008). Stem cells, cell transplantation and liver repopulation. Biochim. Biophys. Acta *1782*, 61–74.

Oka, T., Mazack, V., and Sudol, M. (2008). Mst2 and Lats kinases regulate apoptotic function of Yes kinase-associated protein (YAP). J. Biol. Chem. *283*, 27534–27546.

Ramos, A., and Camargo, F.D. (2012). The Hippo signaling pathway and stem cell biology. Trends Cell Biol. *22*, 339–346.

Sekiya, S., and Suzuki, A. (2012). Intrahepatic cholangiocarcinoma can arise from Notch-mediated conversion of hepatocytes. J. Clin. Invest. *122*, 3914–3918.

Tanigawa, H., Billheimer, J.T., Tohyama, J., Zhang, Y., Rothblat, G., and Rader, D.J. (2007). Expression of cholesteryl ester transfer protein in mice promotes macrophage reverse cholesterol transport. Circulation *116*, 1267–1273.

Tschaharganeh, D.F., Chen, X., Latzko, P., Malz, M., Gaida, M.M., Felix, K., Ladu, S., Singer, S., Pinna, F., Gretz, N., et al. (2013). Yes-associated protein up-regulates Jagged-1 and activates the NOTCH pathway in human hepatocellular carcinoma. Gastroenterology *144*, 1530–1542.e12.

Turner, R., Lozoya, O., Wang, Y., Cardinale, V., Gaudio, E., Alpini, G., Mendel, G., Wauthier, E., Barbier, C., Alvaro, D., and Reid, L.M. (2011). Human hepatic stem cell and maturational liver lineage biology. Hepatology *53*, 1035–1045.

Wu, S., Liu, Y., Zheng, Y., Dong, J., and Pan, D. (2008). The TEAD/TEF family protein Scalloped mediates transcriptional output of the Hippo growth-regulatory pathway. Dev. Cell *14*, 388–398.

Yanger, K., Zong, Y., Maggs, L.R., Shapira, S.N., Maddipati, R., Aiello, N.M., Thung, S.N., Wells, R.G., Greenbaum, L.E., and Stanger, B.Z. (2013). Robust cellular reprogramming occurs spontaneously during liver regeneration. Genes Dev. *27*, 719–724.

Zender, S., Nickeleit, I., Wuestefeld, T., Sörensen, I., Dauch, D., Bozko, P., El-Khatib, M., Geffers, R., Bektas, H., Manns, M.P., et al. (2013). A critical role for notch signaling in the formation of cholangiocellular carcinomas. Cancer Cell *23*, 784–795.

Zhang, L., Ren, F., Zhang, Q., Chen, Y., Wang, B., and Jiang, J. (2008). The TEAD/TEF family of transcription factor Scalloped mediates Hippo signaling in organ size control. Dev. Cell *14*, 377–387.

Zhang, N., Bai, H., David, K.K., Dong, J., Zheng, Y., Cai, J., Giovannini, M., Liu, P., Anders, R.A., and Pan, D. (2010). The Merlin/NF2 tumor suppressor functions through the YAP oncoprotein to regulate tissue homeostasis in mammals. Dev. Cell *19*, 27–38.

Zhao, B., Wei, X., Li, W., Udan, R.S., Yang, Q., Kim, J., Xie, J., Ikenoue, T., Yu, J., Li, L., et al. (2007). Inactivation of YAP oncoprotein by the Hippo pathway is involved in cell contact inhibition and tissue growth control. Genes Dev. *21*, 2747–2761.

Zhao, B., Ye, X., Yu, J., Li, L., Li, W., Li, S., Yu, J., Lin, J.D., Wang, C.-Y., Chinnaiyan, A.M., et al. (2008). TEAD mediates YAP-dependent gene induction and growth control. Genes Dev. *22*, 1962–1971.

Zhou, D., Conrad, C., Xia, F., Park, J.-S., Payer, B., Yin, Y., Lauwers, G.Y., Thasler, W., Lee, J.T., Avruch, J., and Bardeesy, N. (2009). Mst1 and Mst2 maintain hepatocyte quiescence and suppress hepatocellular carcinoma development through inactivation of the Yap1 oncogene. Cancer Cell *16*, 425–438.

Zong, Y., Panikkar, A., Xu, J., Antoniou, A., Raynaud, P., Lemaigre, F., and Stanger, B.Z. (2009). Notch signaling controls liver development by regulating biliary differentiation. Development *136*, 1727–1739.